PCCP

Accepted Manuscript

ROYAL SOCIETY OF CHEMISTRY

www.rsc.org/pccp

Journal Name

ARTICLE

Electrochemical oxidation of 2–propanol over platinum and palladium electrodes in alkaline media studied by in situ attenuated total reflection infrared spectroscopy

Takeou Okanishi,[*a] Yu Katayama,[a] Ryota Ito,[a] Hiroki Muroyama,[a] Toshiaki Matsui[a] and Koichi Eguchi[*a]

The electrochemical oxidation of 2–propanol over Pt and Pd electrodes was evaluated in alkaline media. Linear sweep voltammograms (LSVs), chronoamperograms (CAs), and simultaneous time–resolved attenuated total reflection infrared (ATR–IR) spectra of both electrodes were obtained in a 0.25 M KOH solution with 1 M 2–propanol. The onset potential of the 2–propanol oxidation for Pt was lower than that for Pd in LSVs while the degree of performance degradation for Pd was significantly smaller than that for Pt in CAs. The main product of 2–propanol oxidation was acetone for both electrodes and, only on Pt, acetone produced was catalytically oxidized to enolate ion, which was accumulated on the Pt surface, leading to the significant performance degradation. Carbon dioxide and carbonate species (CO_3^{2-}, HCO_3^-) were not observed during the 2–propanol oxidation for both electrodes, indicating that the complete oxidation of 2–propanol to CO_2 will be a minor reaction.

1. Introduction

Low–molecular weight alcohols have interesting properties as fuels due to their high volumetric energy density and ease in handling, storage, and transportation, compared to those of hydrogen gas. Direct alcohol fuel cells (DAFCs) have been mainly developed with acidic proton exchange membranes such as Nafion®.[1,2] However, in acidic electrolytes, the oxidation reactions of low–molecular weight alcohols are kinetically hindered and require high overpotentials.[3,4] Moreover, rare and expensive Pt is considered to be the best monometallic electrocatalyst for their oxidation reactions in acidic conditions.[3,5] One promising approach to improve alcohol oxidation kinetics is using alkaline media, where overpotentials can be significantly lowered.[6,7] Tripkovic et al. reported that the activity of Pt for methanol oxidation was a strong function of pH of solution and the kinetics at low overpotential was much faster in the alkaline solution than in the acid solution; at 333 K, a factor of 30 at 0.5 V vs. reversible hydrogen electrode (RHE)[6]. Lai et al. also showed a considerable increase in the ethanol oxidation current on a Pt electrode in a 0.1 M NaOH solution as well as a negative shift of ca. 100 mV in the onset potential as compared with that in a 0.1 M HClO₄ solution.[7] Furthermore, an advantage of using alkaline media is the potential use of non–Pt catalysts, such as Pd, Au, and Ni, in DAFC anodes.[8-18] In particular, Pd is well known as an active

electrocatalyst for ethanol oxidation reaction[14-18] as well as methanol oxidation reaction[8-11] in alkaline media.

The electrochemical oxidation of C₃ alcohols, such as 1–propanol and 2–propanol, has been studied less intensively than that of methanol and ethanol. If C₃ alcohols were electrochemically oxidized to CO_2 via dehydrogenation reactions and C–C bond cleavage, huge electrical energy can be obtained using DAFCs. However, in fact, the performance of C₃ alcohols in DAFCs is insufficient compared to that of shorter chain alcohols.[2] Therefore, the oxidation reactions of C₃ alcohols are important for comprehending the influence of the number of C–C bonds on the reaction characteristics.

2–propanol is an interesting fuel because it has some excellent properties in comparison with methanol: (*i*) low toxicity; (*ii*) high boiling point; and (*iii*) low permeability through an electrolyte membrane.[19] The electrochemical oxidation of 2–propanol on Pt in acidic media has been investigated by many groups.[20-29] Sun et al. reported that the 2–propanol oxidation on a Pt electrode could take place immediately when the potential was higher than 0.0 V vs. a saturated calomel electrode in a 0.05 M H₂SO₄ solution.[25] Moreover, several groups found that the majority intermediate in the 2–propanol oxidation over Pt was acetone, and CO_2 was detected as the final oxidation product, using Fourier transform infrared (FT–IR) spectroscopy[24-28] and differential electrochemical mass spectrometry (DEMS).[28] Although the activity and the reaction mechanism of the 2–propanol oxidation on Pt in acidic media have been clarified to some extent, there are few studies on the 2–propanol oxidation in alkaline media.

a. Department of Energy and Hydrocarbon Chemistry, Graduate School of Engineering, Kyoto University, Nishikyo-ku, Kyoto 615-8510, Japan. E-mail: okanishi.takeou.7n@kyoto-u.ac.jp; eguchi@scl.kyoto.u.ac.jp; Fax: +81-75-383-2871; +81-75-383-2510; Tel: +81-75-383-2871; +81-75-383-2519

In the present study, the electrochemical oxidation of 2–propanol over Pt and Pd electrodes in an alkaline aqueous solution was investigated using linear sweep voltammetry, chronoamperometry, and in situ attenuated total reflection infrared (ATR–IR) spectroscopy. The ATR–IR spectroscopy permits high surface sensitivity and unobstructed mass transport on electrodes and thus is promising for the detailed study of the surface oxidation reaction of 2–propanol on Pt and Pd in an alkaline aqueous solution.[30,31] Actually, this measurement technique has been applied for in situ observation of the electrochemical oxidation of CO, alcohols, and ammonia.[9,18,32] The aim of this study is to identify the adsorbed intermediates and the products during the 2–propanol oxidation over Pt and Pd electrodes for the deep understanding of the reaction mechanism. Furthermore, the 2–propanol oxidation activity of Pt and Pd in an alkaline aqueous solution was compared each other.

2. Experimental

For the ATR–IR spectoscopy and the electrochemical measurements, Pt and Pd electrodes were prepared on the Si hemispherical prism (11 mm in radius) by the electroless plating method, which has been described previously in details.[30,33] The Si prism was polished sequentially by 1.0 μm and 0.125 μm diamond suspension and 0.05 μm alumina suspension, and then the smooth surface was etched by 40wt.% NH_4F (98.5%, Wako pure chemical). Subsequently, Pd was deposited on the Si surface by contacting with 0.5 mM $PdCl_2$ (Wako pure chemical)–1% HF (Morita chemical industries) for 5 min to improve the adhesion of Pt and Pd electrode films to the Si surface.[34] For the Pt electrode, after rinsing with ultrapure water (Millipore, Milli–Q), Pt was deposited on the Pd layer with immersing the prism in the plating bath filled with the mixture of the following reagents at 50°C for 30 min; 30 ml of LECTROLESS Pt100 basic solution (Tanaka Kikinzoku Kogyo), 0.6 ml of LECTROLESS Pt100 reducing solution (Tanaka Kikinzoku Kogyo), 30 ml of ultrapure water, and 3 ml of ammonia solution (Wako Pure Chemical). For the Pd electrode, the electroless plating was conducted at 55°C for 4 min using following reagents for the plating bath; 30 ml of LECTROLESS Pd2000S basic solution (Tanaka Kikinzoku Kogyo), 1.5 ml of LECTROLESS Pd2000S additive (Tanaka Kikinzoku Kogyo), 0.6 ml of LECTROLESS Pd1000 reducing powder (Tanaka Kikinzoku Kogyo), and 30 ml of ultrapure water.

All electrochemical measurements were performed in the three–electrode cell made of Teflon according to the previous report.[33] The Pt or the Pd film electrode on Si prism was applied as a working electrode. Platinum wire and Ag/AgCl electrode were used as the counter electrode and the reference electrode, respectively. However, all potentials in this study refer to that of the reversible hydrogen electrode (RHE). An O–ring (15 mm in diameter) was used to fit the prism on the electrochemical cell, and the geometrical Pt surface area contacting with the electrolyte was 1.77 cm^2. Au–plated Cu was applied as a current collector. The supporting electrolyte was 0.25 M KOH prepared from KOH (Sigma-Aldrich, >85 wt.%) and ultrapure water. For 1 M 2–propanol–0.25 M KOH and 1 M acetone–0.25 M KOH, and 1 M acetone triply labelled with ^{13}C (^{13}C acetone)–0.25 M KOH solutions, the desired amount of 2–propanol (Wako Pure Chemical, analytical grade), acetone (Wako Pure Chemical,

analytical grade), and ^{13}C acetone (Cambridge Isotopes, 99 mol%) was also added into the KOH electrolyte solution, respectively. After the electrochemical cell was purged for 30 min with Ar, the working electrodes were electrochemically cleaned by potential cycles in the range of 0.0–1.1 V vs. RHE with a scanning rate of 200 mV sec^{-1}. Each electrochemical measurement was conducted using a potentiostat (Hokuto Denko, HSV100). The linear sweep voltammograms (LSVs) were recorded between 0.05 and 1.10 V vs. RHE at 25°C. The chronoamperograms (CAs) were obtained at 0.6 V for 15 min at 25°C.

The infrared spectrometer (Thermo Fisher Scientific, NICOLET8700) with a liquid nitrogen cooled MCT detector was used for in situ ATR–IR spectroscopy. Instrument parameters were as follows: Incident angle, 70°; spectral resolution, 4 cm^{-1}; time resolution, 4 sec; cumulative number, 20. The experiments were performed at 25°C and 1 atm. The absorbance was calculated as $A = -\log (I/I_0)$, where I_0 and I represent the intensity of the spectra in 0.25 M KOH at 0.05 V vs. RHE and the measured intensity in each experimental condition, respectively.
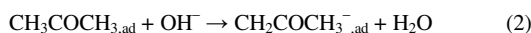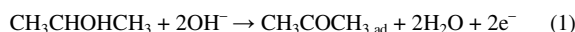
3. Results and discussion

3.1. Electrochemical oxidation of 2–propanol and adsorbed species on the Pt electrode

The electrochemical oxidation of 2–propanol over the Pt film electrode was studied using linear sweep voltammetry in an alkaline aqueous solution containing 2-propanol. Figure 1 shows the LSVs for the Pt film electrode in the absence and presence of 1 M 2–propanol in 0.25 M KOH at a scanning rate of 20 mV s^{-1}. The dashed and solid lines correspond to the results in the absence and presence of 2–propanol, respectively. The onset potential for 2–propanol oxidation was 0.25 V, which was comparable to the results in the acidic conditions as reported before.[25,28] The oxidation current of 2–propanol reached a peak at ca. 0.6 V and the current value was almost maintained with a rise in potential above 0.6 V. One plausible reason for this is a catalyst poisoning by oxidation products of 2–propanol. In addition, the influence of formation of Pt surface oxygen species under the high potential region can be considered as the reason.

Figure 2 displays the time–resolved IR spectra of the Pt film electrode measured sequentially during the linear sweep voltammetry in the presence of 1 M 2-propanol in 0.25 M KOH. The assignment of each peak with wavenumber is summarized in Table 1. A negative–going band at 1620 cm^{-1} is assigned to the bending mode of water and its intensity increased negatively with a rise in potential. This indicates that the water on the Pt surface was partially removed from the surface by another adsorbed species, which was probably OH_{ad}, during the potential sweep.[30,33,35] When the potential was lower than the onset potential of 2-propanol (< 0.25 V), there were no definite peaks in the spectra. However, two characteristic absorption bands appeared at 1497–1507 cm^{-1} and 1699 cm^{-1} above 0.3 V. The band intensity at 1699 cm^{-1} reached the local maximum value at 0.7 V and faded out above 0.8 V where the oxidation current of 2–propanol decreased abruptly. In contrast, the band at 1497–1507 cm^{-1} still existed above 0.8 V and shifted to higher wavenumber with a rise in potential. The Stark effect will be the reason for this band shift, which is induced by the electric field at the

electrode/electrolyte interface, the back–donation of the charge from the metal to the adsorbed species, and the change in the lateral interaction between the adsorbed species.[36-38] Therefore, we can expect that these two bands were well–associated with the 2–propanol oxidation. The band at 1699 cm^{-1} and 1497–1507 cm^{-1} can be ascribable to the C=O stretching mode of acetone and the C–C–O$^-$ stretching mode of enolate ion, respectively.[22,25,39] In ATR–IR, only the molecular vibrations that have dipole changes normal to the surface give absorption. On the basis on the surface selection rule, the adsorbate vibrations of acetone and enolate ion (C=O and C–C–O$^-$ stretching) are normal to the Pt surfaces. Equation (1) and (2) show the electrochemical dehydrogenation of 2–propanol to acetone and the catalytic conversion of acetone to enolate ion, respectively.

$$CH_3CHOHCH_3 + 2OH^- \rightarrow CH_3COCH_{3,ad} + 2H_2O + 2e^- \quad (1)$$

$$CH_3COCH_{3,ad} + OH^- \rightarrow CH_2COCH_3^-{}_{,ad} + H_2O \quad (2)$$

In addition, the band at 1600cm^{-1} may be due to *ir* absorption by species from dehydration of 2–propanol.[27] Moreover, a slight absorption displayed in the spectrum around 1570 cm^{-1}. This band may be ascribable to the C=O stretching of mesityl oxide, which can be produced via aldol–condensation–like surface reactions of acetone.[39] However, actually these bands are not clear.

In acidic conditions, the major product in 2–propanol oxidation on Pt was acetone, as in the literatures.[24-26] Furthermore, it was also reported that a small quantity of CO_2 was detected as the final oxidation product, which was an evidence of the complete oxidation of 2–propanol on Pt.[24-26] In contrast, interestingly, adsorbed enolate ion as well as acetone was detected under an alkaline condition in this study. If 2–propanol was completely oxidized to CO_2 on Pt electrode in alkaline media, absorption peaks related to the OCO asymmetric stretching mode of CO_2 at ca. 2340 cm^{-1}, CO_3^{2-} at ca. 1390 cm^{-1} and HCO_3^- at ca. 1360 cm^{-1} would be observed.[9,40,41] Moreover, the symmetric and the asymmetric bending modes of CH_3 in acetone exhibit the absorbance at ca. 1350–1450 cm^{-1}, which will be discussed later in the section on adsorption and conversion of acetone on Pt and Pd electrodes.[27] However, there were no obvious peaks attributable to these vibration modes; although several peaks appears to be at 1350–1450 cm^{-1}, their intensity was independent of the applied potential. Thus, it is difficult to distinguish the characteristic bands related to carbonate species from these bands even if these species existed on the electrode. Anyway, if CO_2 and/or carbonate species were produced through the 2-propanol oxidation in the present study, the amount of them should be negligible. Furthermore, no bands corresponding to adsorbed CO were observed in the IR spectra. This is a direct proof that 2–propanol cannot dissociate into CO on the Pt electrode in an alkaline aqueous solution. Therefore, we propose that the main product of 2–propanol oxidation is enolate ion as well as acetone and the complete oxidation of 2–propanol scarcely occurrs on the Pt electrode in an alkaline media.

3.2. Electrochemical oxidation of 2–propanol and adsorbed species on the Pd electrode

Figure 3 shows the LSVs for the Pd film electrode in the absence and presence of 1 M 2–propanol in 0.25 M KOH at a scanning rate

of 20 mV s^{-1}. The dashed and solid lines correspond to the results in the absence and presence of 2–propanol, respectively. The onset potential for 2–propanol oxidation was 0.37 V, which was higher than that for the Pt electrode (0.20 V). The oxidation current reached a peak at 0.83 V and then significantly decreased above this potential. The reasons for this behavior are probably similar to those for the Pt electrode, as discussed above.

Figure 4 displays the time–resolved IR spectra of the Pd film electrode measured sequentially during the linear sweep voltammetry in the presence of 1 M 2–propanol in 0.25 M KOH. Two main bands at 1620 cm^{-1} and 1699 cm^{-1} are assigned to the bending mode of water and the C=O stretching mode of acetone, respectively, as in the case of Fig. 2. The intensity of the band at 1699 cm^{-1} increased from 0.4 V and its local maximum value was achieved at 0.9 V. This result is consistent with the electrochemical oxidation behavior of 2–propanol on the Pd electrode, as shown in Fig. 3. Note that the band at 1497–1507 cm^{-1} related to enolate ion was not observed on the Pd electrode in contrast to the result for the Pt electrode. In addition, no obvious bands corresponding to CO_2, CO_3^{2-}, HCO_3^-, and CO, which can be the evidence of the complete oxidation of 2–propanol, were observed in the IR spectra of the Pd electrode. This result agreed with that for the Pt electrode. Therefore, it can be considered that 2–propanol was oxidized to acetone and any subsequent reactions including the complete oxidation scarcely occurred on the Pd electrode in an alkaline media.

3.3. Oxidation of 2–propanol at the constant potential

In order to investigate in detail the adsorption behavior of acetone and enolate ion during the 2–propanol oxidation, chronoamperometric measurements and simultaneous time–resolved ATR–IR spectroscopy were performed for the Pt and Pd film electrodes in the presence of 1 M 2–propanol in 0.25 M KOH. Figure 5 shows the time course of current obtained at 0.6 V and the peak intensity of the bands at 1497–1507 cm^{-1} and 1699 cm^{-1} for each electrode. The current value for Pt after 1min duration was 0.86 mA, which was higher than that for Pd of 0.60 mA. After 15 min duration, however, the current value for Pt (0.23 mA) was reduced by ca. 73% as compared with that after 1 min. In the case of Pd, the decline rate was ca. 50% (from 0.60 to 0.30 mA). These results indicate that the degree of performance degradation for Pd was significantly smaller than that for Pt. The band intensity at 1699 cm^{-1} related to acetone remained almost unchanged for both electrodes during the analysis. At the same time, the band intensity at 1497–1507 cm^{-1} related to enolate ion, which was observed on only Pt, gradually increased. These findings revealed that 2–propanol was oxidized to acetone through the dehydrogenation reaction on both Pt and Pd electrodes and the coverage of adsorbed acetone was constant at 0.6 V. Moreover, the produced acetone was found to be catalytically oxidized to enolate ion, which was accumulated on only Pt during the 2–propanol oxidation. Therefore, it is reasonable to consider that the accumulation of produced enolate ion on the Pt surface is responsible for the significant decrease in the oxidation current of 2–propanol on the Pt electrode.

3.4. Adsorption and conversion of acetone on Pt and Pd electrodes

To ensure that the characteristic band at 1699 cm^{-1} was related to acetone and enolate ion was produced on only Pt, linear sweep voltammetry and simultaneous time–resolved ATR–IR spectroscopy were examined for the Pt and Pd electrodes in the presence of 1 M acetone in 0.25 M KOH. Figure 6 shows the LSVs for the Pt film electrodes in the absence and presence of 1 M acetone in 0.25 M KOH at a scanning rate of 20 mV s^{-1}. The dashed and solid lines correspond to the results in the absence and presence of acetone, respectively. Figure 7 displays the time–resolved IR spectra of the Pt film electrode measured sequentially during the linear sweep voltammetry in the presence of acetone in 0.25 M KOH. The band assignment is also listed in Table 1. The LSV in the acetone–containing solution apparently was different from that in the acetone–free solution. The hydrogen desorption peak at approximately 0.05–0.40 V as well as the double–layer region at approximately 0.40–0.60 V was diminished in presence of acetone. In addition, a slight oxidation current was observed above 0.6 V. Bänsch et al. reported that in acidic environment, acetone adsorbed on Pt in the double–layer region as well as the hydrogen desorption region, leading to the reduction in current.[42] They also reported that the oxidation reaction of acetone to CO_2 occurred at the OH adsorption region. In this study, it is reasonable to consider that acetone strongly adsorbed on the Pt surface and was oxidized in an alkaline aqueous solution. However, the oxidation current of acetone was significantly lower than that of 2–propanol (see Fig. 1) and no characteristic bands related to CO_2 and carbonate species were detected in the simultaneous IR spectra of the Pt electrode as shown in Fig. 7. Actually, the C=O stretching mode at 1704 cm^{-1}, the CH$_3$ symmetric bending mode at 1368 cm^{-1}, and the CH$_3$ asymmetric bending mode at 1440 cm^{-1} related to acetone on the Pt surface were observed in the spectra.[27] Furthermore, the C–C–O$^-$ stretching band of enolate ion at 1490–1560 cm^{-1} appeared in the spectra. These results strongly support that 2-propanol was oxidized to acetone and subsequently acetone produced was conversed to enolate ion on the Pt electrode in alkaline media.

To confirm the band assignment related to acetone and enolate ion, linear sweep voltammetry and simultaneous time–resolved ATR–IR spectroscopy were carried out for the Pt electrode in the presence of 1 M ^{13}C acetone in 0.25 M KOH. As shown in Fig. S1, all the bands except that of HOH bend of water showed the isotope effect. In fact, in 1M ^{13}C acetone–0.25 M KOH, each peak related to acetone and enolate ion negatively shifted by 4-10 cm^{-1} compared that in 1 M acetone–0.25 M KOH. This result supports the band assignment shown in Table 1.

Figure 8 shows the LSVs for the Pd film electrode in the absence and presence of 1 M acetone in 0.25 M KOH at a scanning rate of 20 mV s^{-1}. The dashed and solid lines correspond to the results in the absence and presence of acetone, respectively. Figure 9 displays the time–resolved IR spectra of the Pd film electrode measured sequentially during the linear sweep voltammetry in the presence of acetone in 0.25 M KOH. The band assignment is also listed in Table 1. Similar to the Pt results, the LSV of the Pd electrode in the acetone–containing solution obviously changed compared to that in the acetone–free solution and showed an oxidation current above ca. 0.7 V, which was much smaller than that for the 2–propanol oxidation (see Fig. 3). For the IR spectra as shown in Fig. 9, three characteristic bands related to acetone appeared at 1362, 1450, and

1700 cm^{-1}. In addition, a slight broad peak at 1550 cm^{-1} came out above ca. 0.8 V, which was probably related to enolate ion and its intensity was much smaller than that for Pt electrode. In fact, enolate ion was not detected on the Pd surface during the 2–propanol oxidation. This will be due to the small amount of acetone adsorbed on the Pd surface above 0.8 V during the 2–propanol oxidation. Therefore, these results clarified the adsorption and the conversion behavior of acetone on the electrodes and contributed to the further comprehension of the reaction mechanism of the 2–propanol oxidation in alkaline media.

4. Conclusions

The electrochemical oxidation of 2–propanol over Pt and Pd electrodes in the alkaline aqueous solution was investigated by electrochemical measurements and in situ ATR–IR spectroscopy. The onset potential of the 2–propanol oxidation for Pt was lower than that for Pd in LSVs while the degree of performance degradation for Pd was significantly smaller than that for Pt in CAs. The main product of 2–propanol oxidation was acetone for both electrodes and, only on Pt, acetone produced was catalytically oxidized to enolate ion. Moreover, the accumulation of produced enolate ion caused the significant decrease in the oxidation current of 2–propanol on the Pt electrode. The complete oxidation of 2-propanol to CO_2 will be a minor reaction because CO_2 and carbonate species were not observed during the 2–propanol oxidation and the acetone oxidation for both electrodes.

Acknowledgements

Notes and references

1   A. Heinzel and V. M. Barragán, *J. Power Sources*, 1999, **84**, 70-74.
2   C. Lamy, A. Lima, V. LeRhun, F. Delime, C. Coutanceau and J. M. Léger, *J. Power Sources*, 2002, **105**, 283-296.
3   E. Antolini, *J. Power Sources*, 2007, **170**, 1-12.
4   F. Vigier, C. Coutanceau, A. Perrard, E. M. Belgsir and C. Lamy, *J. Appl. Electrochem.*, 2004, **34**, 439-446.
5   F. Vigier, S. Rousseau, C. Coutanceau, J.-M. Leger and C. Lamy, *Top. Catal.*, 2006, **40**, 111-121.
6   A. V. Tripković, K. D. Popović, B. N. Grgur, B. Blizanac, P. N. Ross and N. M. Marković, *Electrochim. Acta*, 2002, **47**, 3707-3714.
7   S. C. S. Lai, S. E. F. Kleijn, F. T. Z. Öztürk, V. C. van Rees Vellinga, J. Koning, P. Rodriguez and M. T. M. Koper, *Catal. Today*, 2010, **154**, 92-104.
8   C. Xu, L. Cheng, P. Shen and Y. Liu, *Electrochem. Commun.*, 2007, **9**, 997-1001.
9   Y. Y. Yang, J. Ren, H. X. Zhang, Z. Y. Zhou, S. G. Sun and W. B. Cai, *Langmuir*, 2013, **29**, 1709-1716.

10 C. Bianchini and P. K. Shen, *Chem. Rev.*, 2009, **109**, 4183-4206.

11 C. Xu, Z. Tian, P. Shen and S. P. Jiang, *Electrochim. Acta*, 2008, **53**, 2610-2618.

12 J. Hernández, J. Solla-Gullón, E. Herrero, A. Aldaz and J. M. Feliu, *Electrochim. Acta*, 2006, **52**, 1662-1669.

13 E. Antolini and E. R. Gonzalez, *J. Power Sources*, 2010, **195**, 3431-3450.

14 Z. X. Liang, T. S. Zhao, J. B. Xu and L. D. Zhu, *Electrochim. Acta*, 2009, **54**, 2203-2208.

15 Z.-Y. Zhou, Q. Wang, J.-L. Lin, N. Tian and S.-G. Sun, *Electrochim. Acta*, 2010, **55**, 7995-7999.

16 Z. Zhang, L. Xin, K. Sun and W. Li, *Int. J. Hydrogen Energy*, 2011, **36**, 12686-12697.

17 S. Sun, Z. Jusys and R. J. Behm, *J. Power Sources*, 2013, **231**, 122-133.

18 Y.-Y. Yang, J. Ren, Q.-X. Li, Z.-Y. Zhou, S.-G. Sun and W.-B. Cai, *ACS Catal.*, 2014, **4**, 798-803.

19 D. Cao and S. H. Bergens, *J. Power Sources*, 2003, **124**, 12-17.

20 S. N. Raicheva, M. V. Christov and E. I. Sokolova, *Electrochim. Acta*, 1981, **26**, 1669-1676.

21 P. T. A. Sumodjo, E. J. d. Silva and T. Rabockai, *J. Electroanal. Chem.*, 1989, **271**, 305-317.

22 L.-W. H. Leung and M. J. Weaver, *Langmuir*, 1990, **6**, 323-333.

23 P. Gao, C.-H. Lin, C. Shannon, G. N. Salaita, J. H. White, S. A. Chaffins and A. T. Hubbard, *Langmuir*, 1991, **7**, 1515-1524.

24 L.-W. H. Leung, S.-C. Chang and M. J. Weaver, *J. Electroanal. Chem.*, 1989, **266**, 317-336.

25 S.-G. Sun, D.-F. Yang and Z.-W. Tian, *J. Electroanal. Chem.*, 1990, **289**, 177-187.

26 S.-G. Sun and Y. Lin, *J. Electroanal. Chem.*, 1994, **375**, 401-404.

27 S.-G. Sun and Y. Lin, *Electrochim. Acta*, 1996, **41**, 693-700.

28 E. Pastor, S. González and A. J. Arvia, *J. Electroanal. Chem.*, 1995, **395**, 233-242.

29 E. I. Sokolova and M. V. Christov, *J. Electroanal. Chem.*, 1984, **175**, 195-205.

30 A. Miki, S. Ye and M. Osawa, *Chem. Comm.*, 2002, 1500-1501.

31 M. Osawa, *Bull. Chem. Soc. Japan*, 1997, **70**, 2861-2880.

32 K. Kunimatsu, T. Sato, H. Uchida and M. Watanabe, *Electrochimica Acta*, 2008, **53**, 6104-6110.

33 T. Matsui, S. Suzuki, Y. Katayama, K. Yamauchi, T. Okanishi, H. Muroyama and K. Eguchi, *Langmuir*, 2015, **31**, 11717-11723.

34 S. Karmalkar and J. Banerjee, *J. Electrochem. Soc.*, 1999, **146**, 580-584.

35 G. Samjeské, K. Komatsu and M. Osawa, *J. Phys. Chem. C*, 2009, **113**, 10222-10228.

36 M. J. Weaver, S. Zou and C. Tang, *J. Chem. Phys.*, 1999, **111**, 368-381.

37 F. M. Hoffmann, *Surf. Sci. Rep.*, 1983, **3**, 107-192.

38 Y. J. Chabal, *Surf. Sci. Rep.*, 1988, **8**, 211-357.

39 M. I. Zaki, M. A. Hasan and L. Pasupulety, *Langmuir*, 2001, **17**, 768-774.

40 A. Berná, A. Rodes and J. M. Feliu, *J. Phys. Chem. B*, 2004, **108**, 17928-17939.

41 H. Miyake, T. Okada, G. Samjeské and M. Osawa, *Phys. Chem. Chem. Phys.*, 2008, **10**, 3662-3669.

42 B. Bänsch, T. Hartung, H. Bakruschat and J. Heitbaum, *J. Electroanal. Chem.*, 1989, **259**, 207-215.
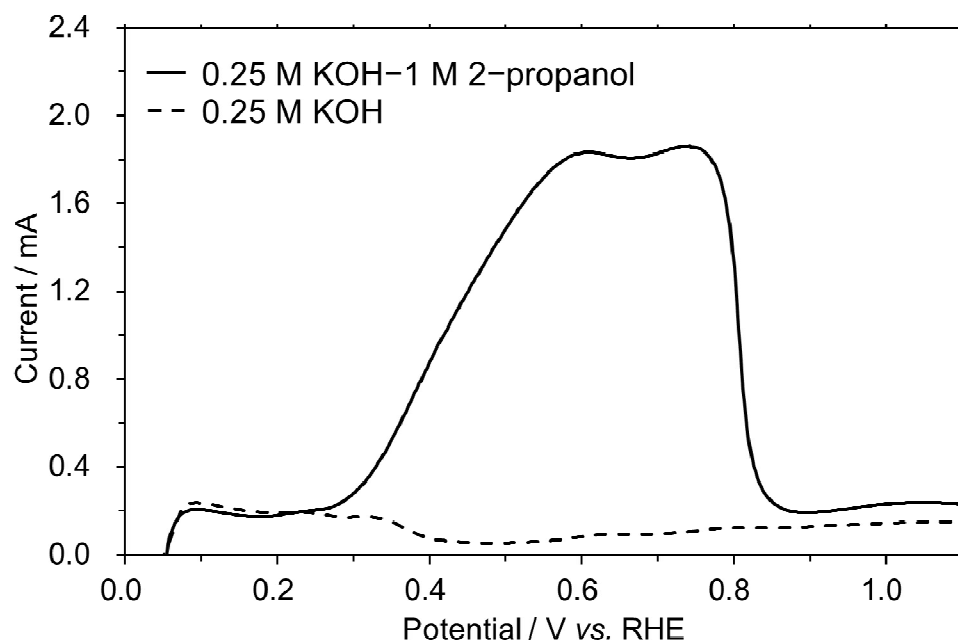
Fig. 1 (T. Okanishi et al.)

Fig. 1. Linear sweep voltammograms of Pt film electrode in the presence (solid line) and absence (dashed) of 1 M 2–propanol in 0.25 M KOH with a scanning rate of 20 mV s^{-1}.
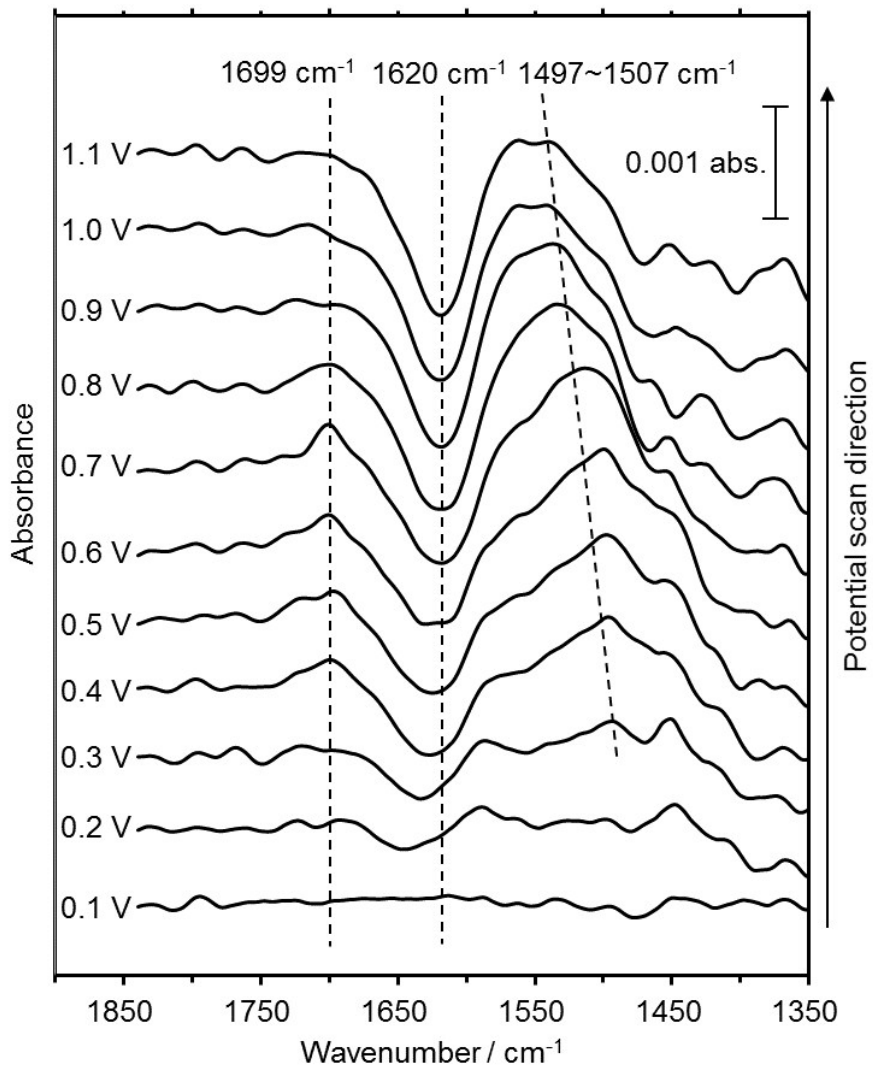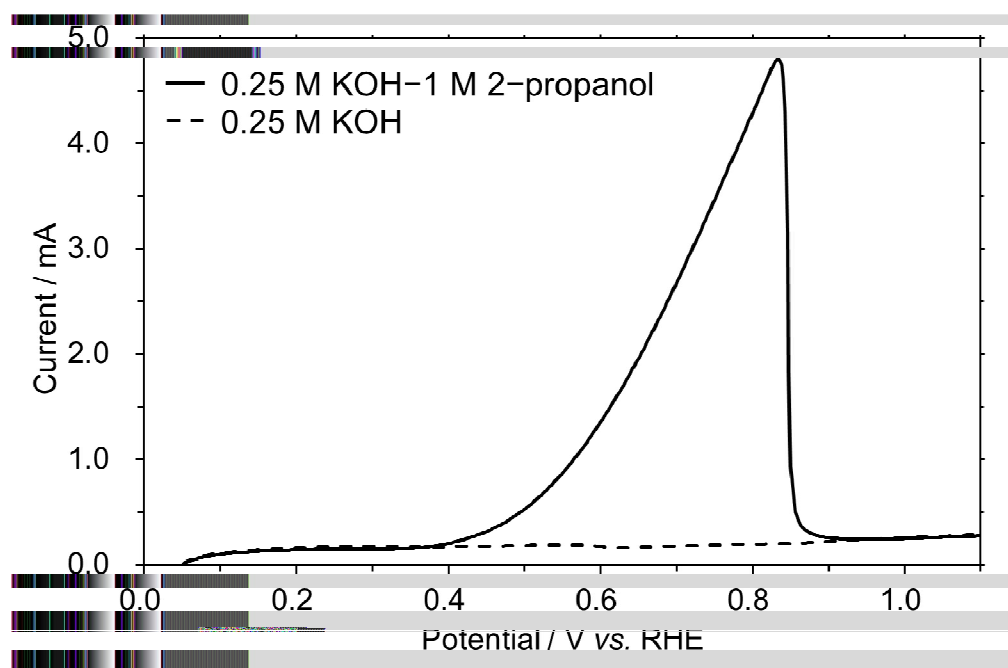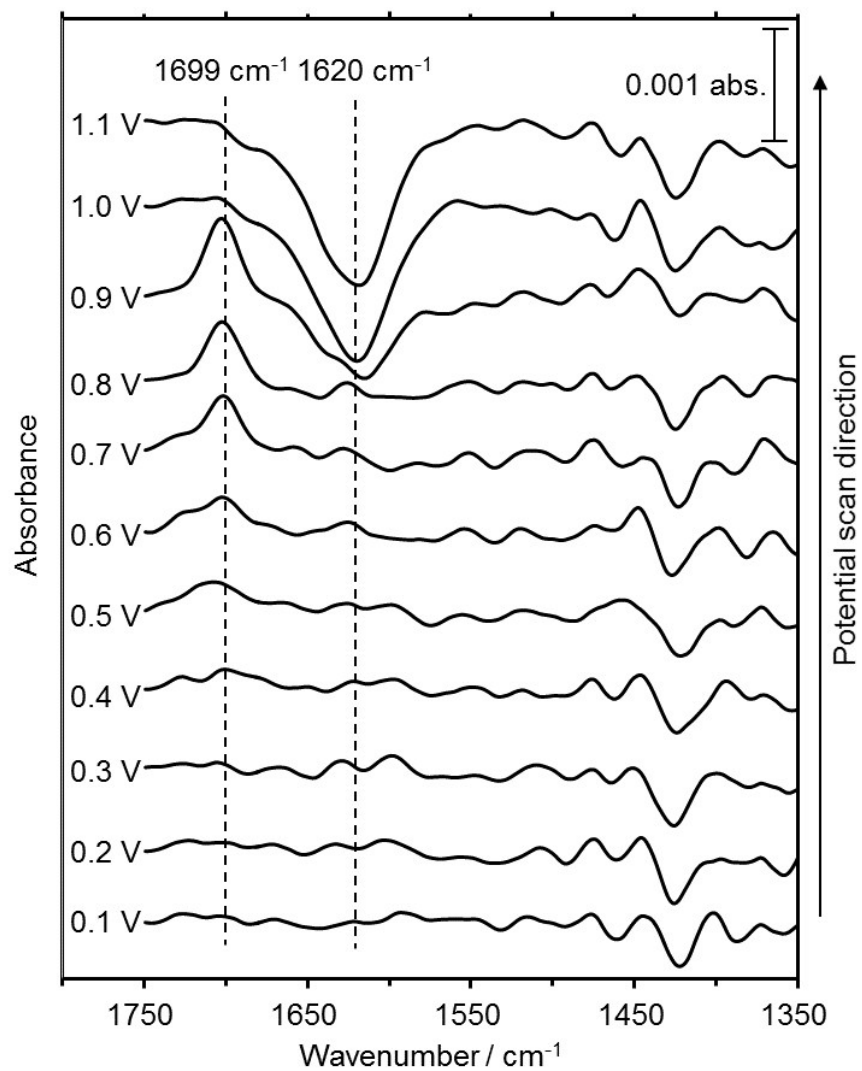
1

Fig. 2 (T. Okanishi et al.)

Fig. 2. Time–resolved IR spectra of the Pt surface acquired simultaneously with the linear sweep voltammogram in 0.25 M KOH solution with 1 M 2–propanol.
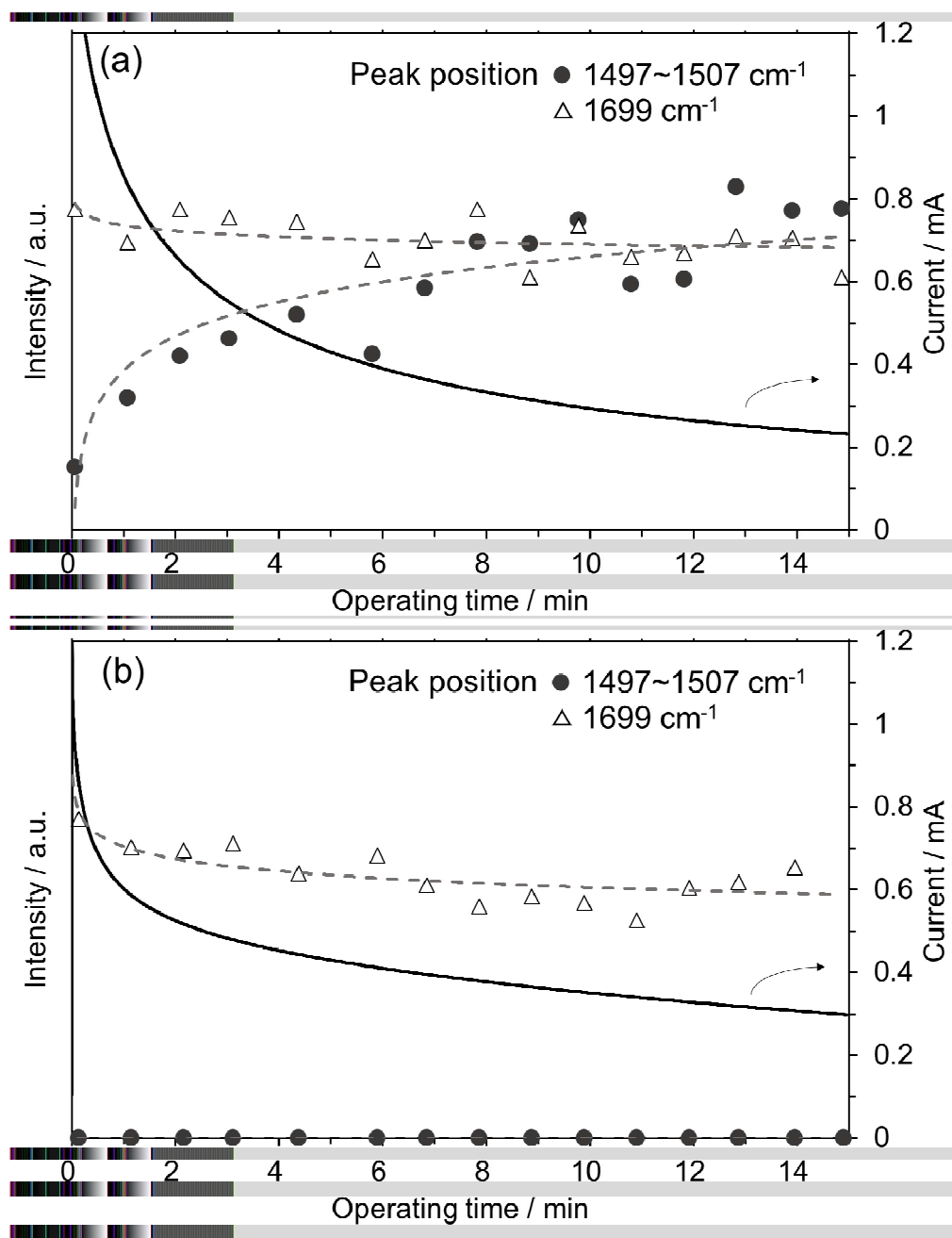
2

Fig. 3 (T. Okanishi et al.)

Fig. 3. Linear sweep voltammograms of Pd film electrode in the presence (solid line) and absence (dashed) of 1 M 2–propanol in 0.25 M KOH with a scanning rate of 20 mV s^{-1}.

3

Fig. 4 (T. Okanishi et al.)

Fig. 4. Time–resolved IR spectra of the Pd surface acquired simultaneously with the linear sweep voltammogram in 0.25 M KOH solution with 1 M 2–propanol.

4

Fig. 5 (T. Okanishi et al.)

Fig. 5. Time cource of 2–propanol oxidation current and the band intensities at 1497–1507 cm^{-1} and 1699 cm^{-1} of (a) Pt and (b) Pd film electrode in 0.25 M KOH with 1 M 2–propanol at the constant potential of 0.6 V vs. RHE.
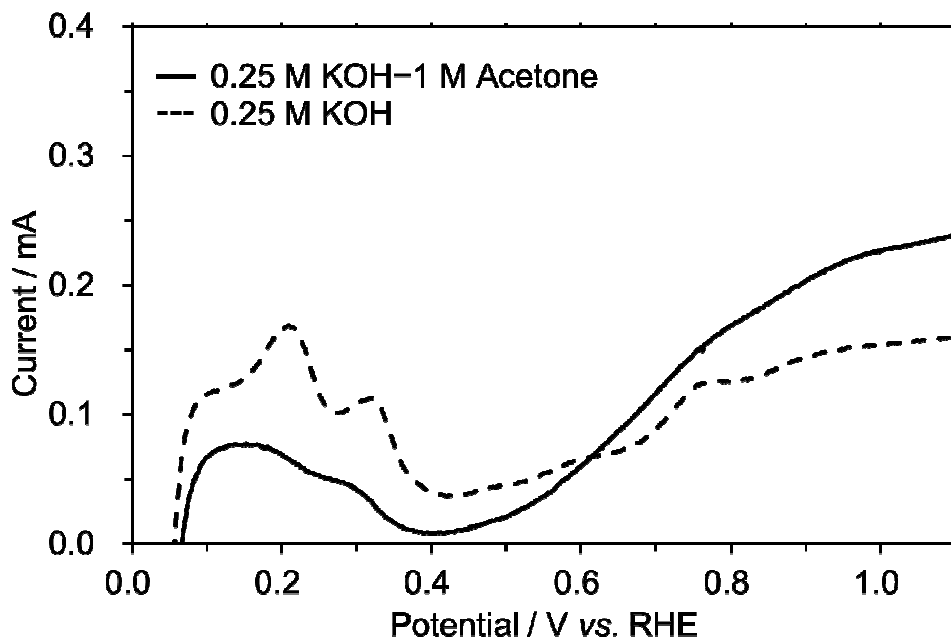
Fig. 6 (T. Okanishi et al.)

Fig. 6. Linear sweep voltammograms of Pt film electrode in the presence (solid line) and absence (dashed) of 1 M acetone in 0.25 M KOH with a scanning rate of 20 mV s^{-1}.
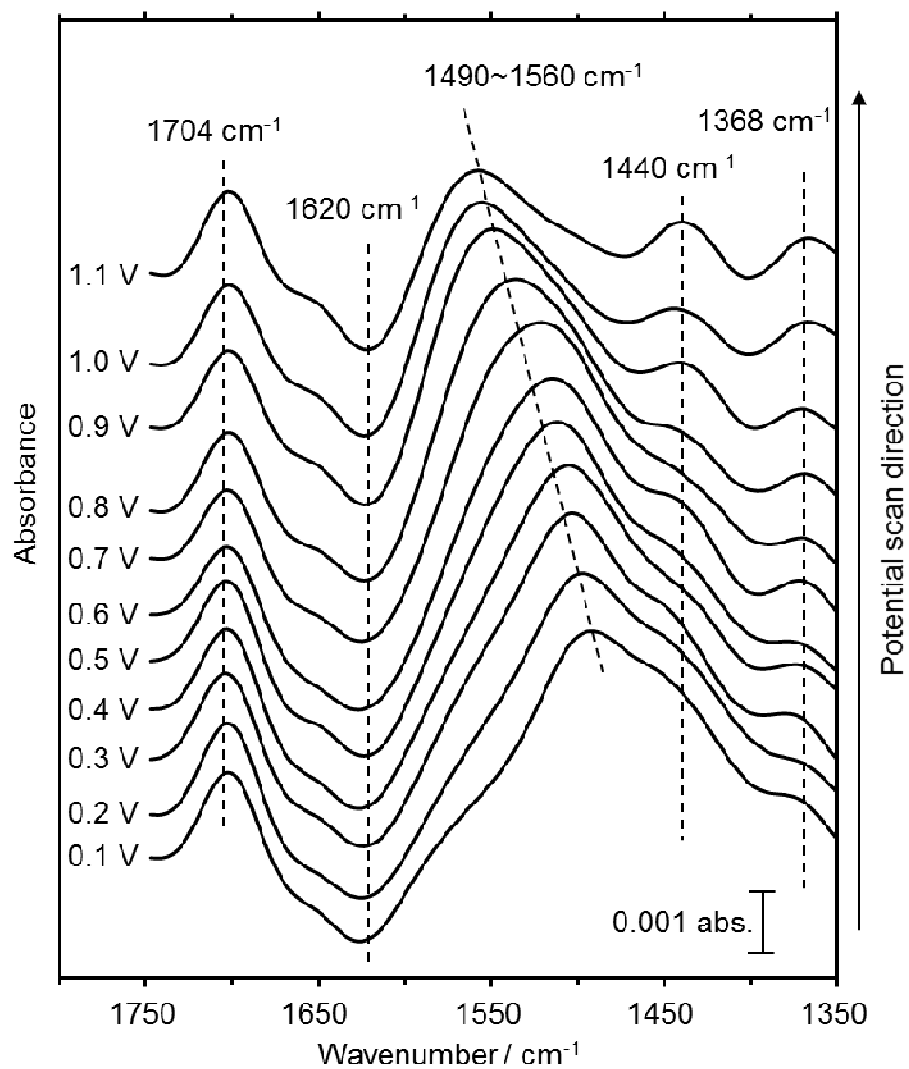
Fig. 7 (T. Okanishi et al.)

Fig. 7. Time–resolved IR spectra of the Pt surface acquired simultaneously with the linear sweep voltammograms in 0.25 M KOH solution with 1 M acetone.
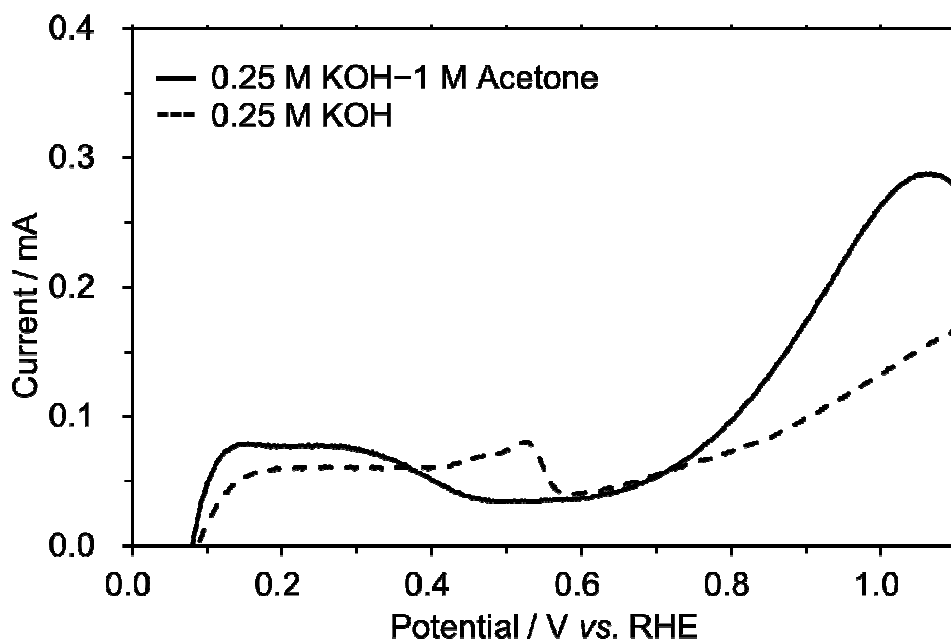
Fig. 8 (T. Okanishi et al.)

Fig. 8. Linear sweep voltammograms of Pd film electrode in the presence (solid line) and absence (dashed) of 1 M acetone in 0.25 M KOH with a scanning rate of 20 mV s^{-1}.
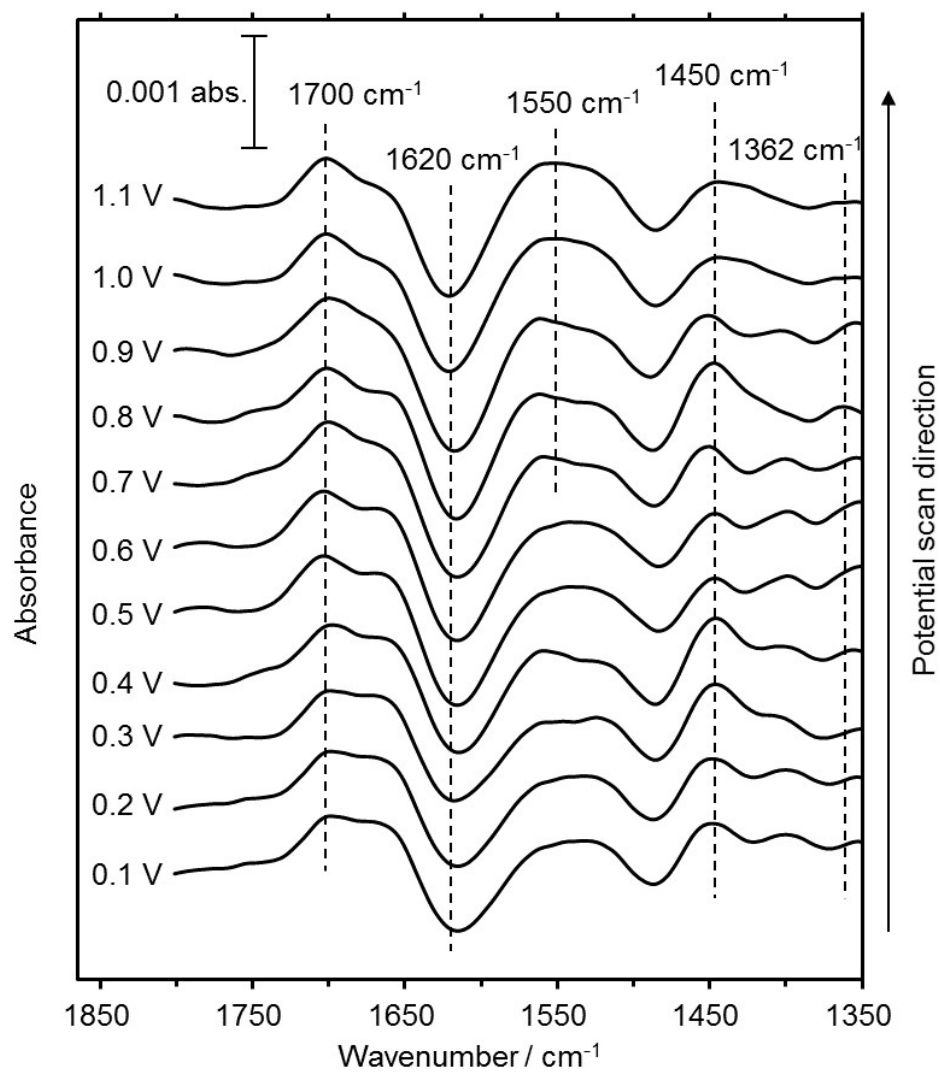
8

Fig. 9 (T. Okanishi et al.)

Fig. 9. Time–resolved IR spectra of the Pd surface acquired simultaneously with the linear sweep voltammograms in 0.25 M KOH solution with 1 M acetone.

Table 1 (T. Okanishi et al.)

Table 1 ATR–IR band assignment in 1 M 2-propanol–0.25 M KOH and 1 M acetone–0.25 M KOH

Wavenumber / cm^{-1}	Assignment	Ref.
1699, 1700, 1704	CO stretch of acetone	[22, 25, 39]
1620	HOH bend of water	[30, 33, 35]
1497-1507, 1490-1560, 1550	C–C–O$^-$ stretch of enolate ion	[39]
1440, 1450	CH$_3$ asymmetric bend of acetone	[27]
1362, 1368	CH$_3$ symmetric bend of acetone	[27]